ICOT/IR/19

icot

A NUMERICAL MODEL TO STUDY TIDES AND SURGES IN A RIVER – SEA COMBINATION

BY

JOYCE E. BANKS

1969

institute of coastal oceanography and tides

NATURAL ENVIRONMENT RESEARCH COUNCIL

A NUMERICAL MODEL TO STUDY TIDES AND SURGES IN A RIVER - SEA COMBINATION

BY

JOYCE E. BANKS

1969

INTERNAL REPORT

Abstract

A finite difference scheme has been devised to accommodate a one-dimensional river model and a two-dimensional sea model in the same computational array. The design of the sea model is based upon a previous formulation by Heaps, but modified to include such non-linear terms as quadratic bottom friction; the river-model, which also uses non-linear hydrodynamic equations, is that established by Rossiter and Lennon (1965). The vital part of the work is the matching of current and elevation values at the common points of the sea and river models. In the numerical computations, carried out by an ALGOL program, the specific case of the Thames-North Sea connection has been considered. A combination of tidal and surge responses may be studied by specifying the initial tidal contours of the sea and the subsequent external influences of (a) tidal oscillation along the open boundary, and (b) wind stress over the area. The variations of the wind stress with time are idealized functions, consequently in this study, no attempt is made to hindcast any actual surge. Computed elevations will be used to produce a co-tidal chart for the M_2 constituent. The program can be used to study the interaction of tides and surges.

A numerical model of the Thames Estuary was formulated at the Tidal Institute three years ago, for the study of tides and surges in the estuary. This model is based on the one-dimensional equations of continuity and motion as follows :

$$\frac{\partial A\bar{q}}{\partial y} = -b\frac{\partial \zeta^{(R)}}{\partial t}$$

$$\frac{\partial \bar{q}}{\partial t} + \bar{q}\frac{\partial \bar{q}}{\partial y} = -g\frac{\partial \zeta^{(R)}}{\partial y} + \frac{S_s}{H\rho} - \frac{S_b}{H\rho} - \frac{gH}{2\rho}\frac{\partial \rho}{\partial y}$$

Here y denotes distance measured along the length of the river, and t the time. The dependent variables for solution are $\zeta^{(R)}$ surface elevation, and $\bar{q}$ mean current over a transverse cross-section directed along the length. Other parameters are A cross-sectional area, b mean surface breadth, H mean depth of water, S_s surface stress, and S_b bottom stress and these are all functions of time and position, ρ is the depth mean water density.

Figure 1 shows a map of the Thames. In the model, elevations are evaluated at the sections marked, and currents at intermediate sections. As boundary conditions, the total flow is specified at the head and elevation at the mouth. The derivatives in the hydrodynamical equations are replaced by central space and time differences and the initial value method is applied to build up numerically the system of elevations and currents from some arbitrary initial state.

Figure 2 shows the pattern of calculation, in which distance along the river is measured horizontally and time vertically. Given currents at the initial time level $-\tau/2$, say, and elevations at time level 0, currents are calculated at the odd time levels $\tau/2, 3\tau/2, 5\tau/2$ using the equation of motion, and elevations at the even time levels $\tau, 2\tau, 3\tau, \ldots\ldots$ using the equation of continuity.

Rossiter, J.R. and Lennon, G.W. : Computation of tidal conditions in the Thames Estuary by the initial value method. Proc. Instn. civ. Engrs., vol. 31, pp 25-56, May 1965.

Heaps, N.S. : A two-dimensional numerical sea model. Tidal Institute, in preparation.

It was desirable to extend the computations to cover both the river and the adjoining North Sea, so that disturbances in the river could be related to tidal conditions in the sea and the meteorological forces acting over the sea. In particular, it was of interest to investigate the effects on the river levels of non-linear interactions between tide and surge in the sea. The possibility of linking dynamically the one-dimensional river model described above with a two-dimensional model of the sea outside was considered. Subsequently, the combined river-sea model shown in figure 3 was devised. The sea area covered was restricted to the southern North Sea in order to limit the size of the computations and then accommodate them within the capacity of the available computer.

A brief description of the finite-difference schemes used in the two-dimensional model for initial-value computations now follows. The two-dimensional differential equations of motion and continuity were expressed with latitude ϕ and longitude χ as independent space co-ordinates, elevation ζ and the components of total flow U, V being the dependent variables. A quadratic law of bottom friction was assumed and the non-linear influence produced by allowing for the total depth $h+\zeta$ at any time was included. Product terms in the acceleration were ignored, the friction of the wind on the sea surface was taken into account, but the effects of atmospheric pressure gradients over the sea were ignored. Following from these assumptions the hydrodynamical equations are expressed as :

$$\frac{\partial \zeta}{\partial t} = -\frac{1}{a\cos\phi}\left[\frac{\partial U\cos\phi}{\partial \phi} + \frac{\partial V}{\partial \chi}\right]$$

$$\frac{\partial U}{\partial t} = -\Omega V - \frac{g}{a}(h+\zeta)\frac{\partial \zeta}{\partial \phi} + \frac{F_s}{\rho} - \frac{k U\sqrt{U^2+V^2}}{(h+\zeta)^2}$$

$$\frac{\partial V}{\partial t} = \Omega U - \frac{g}{a\cos\phi}(h+\zeta)\frac{\partial \zeta}{\partial \chi} + \frac{G_s}{\rho} - \frac{k V\sqrt{U^2+V^2}}{(h+\zeta)^2}$$

Here a is the radius of the earth, $\Omega = 2\omega\sin\phi$ where ω is the angular speed of the earth's rotation about its axis, F_s, G_s are the components of the surface stress in the directions of increasing ϕ, χ respectively, and k is the coefficient of bottom friction.

In replacing these differential equations by difference equations, central space differences were employed and a combination of forward and backward time differences. Thus, knowing elevations and flows at time t the flows at a later time $t+\tau$ were deduced from the equations of motion (incorporating forward time differences). The elevations at time $t+\tau$ were subsequently found from the equation of continuity (incorporating a backward time difference). In this way elevations and total flows at time $t+\tau$ were deduced from those at time t, the transformation thereby providing the necessary step forward in values for the building up in time of the motion in the sea, from some given initial state. Figure 3 shows the deployment of the grid points in the sea : elevation is evaluated at the "circle" points and total flow at the "cross" points. The elevation and stream points form two interlacing nets. Along the closed "coastal" boundaries of the model the condition of zero normal flow is satisfied and along the open boundaries to the north and south tidal elevation is specified as a function of the time.

The connection of the two-dimensional system with the one-dimensional river system is the crucial part of the work. A plan-form diagram of the connection is shown in figure 4. The narrowing of the sea area represents the converging estuary. A width of two mesh lengths is the furthermost limit one can proceed with this narrowing before introducing the line of alternate elevation and current points which represents the river. The one- and two-dimensional arrays coincide at a centrally positioned stream point known as the pivot. Elevational input to the river at the mouth is derived by averaging the two sea elevations on either side of the pivot. Of course, the river motion (as effecting

the current at the pivot) will, conversely, influence the sea elevations and it is this mutual interaction between river and sea which one must try to incorporate in the calculations. For convenience in forming space differences across the pivot, the grid spacing in the sea, along the line of the river, was taken equal to the sectional spacing in the river. The distance between consecutive elevation (or current) points in the river is 4.89 miles and this leads to taking an interval of 6.8° longitude between successive stream or elevation points lying on a parallel of latitude in the sea.

Figure 5 is a three-dimensional diagram showing the time levels at which the elevations and currents in river and sea are evaluated. For the sea, given the state of motion and displacement at $t = 0$, subsequent states of motion and displacement are determined at $t = \tau, 2\tau, 3\tau, \ldots$. For the river, given currents at $t = -\tau/2$ and elevations at $t = 0$, currents are subsequently found at $t = \tau/2, 3\tau/2, 5\tau/2, \ldots$ and elevations at $t = \tau, 2\tau, 3\tau, \ldots\ldots$. Thus, the time-step in the river computations is taken equal to that in the sea computations - both being equal to τ. For the stability of the one-dimensional system it was estimated that $\tau < 10$ mins., and for the stability of the two-dimensional system $\tau < 4$ mins. Therefore for the stability of computations in both systems a time step of 3 min. was used.

Referring to figure 5 a more detailed description is now given of the sequence of calculations in one cycle of the iterative procedure by which the elevations and currents in the river-sea system are built up numerically in time. Suppose that all the elevations and currents are known at the grid points of the two lowest levels ($t = -\tau/2$, $t = 0$) which, when $n = 0$ may be regarded as the initial conditions. The problem, then, is to calculate values at the grid points of the two higher levels $t = \tau/2$ and $t = \tau$. Subsequent repetition of such a procedure produces a step forward in time by calculating values at successive time levels separated by the interval $\tau/2$.

First, using the river equation of motion, the currents at $t = \tau/2$ are calculated - the value at section 1 is obtained from a linear extrapolation.

Next, using the sea equations, elevations and flows over the sea region are calculated at $t = \tau$ from those at $t = 0$. This includes the flow at the pivot, the determination of which involves using the river elevation at the point lying immediately outside the two-dimensional grid system.

An elevation input to the river at $t = \tau$ may now be derived by averaging the two sea elevations on either side of the first river point. Then, by using the river equation of continuity, the entire set of elevations along the river at $t = \tau$ could be determined. However, before proceeding thus, the current at the pivot at $t = \tau$ (determined from the sea difference scheme) is smoothed in relation to the currents at this point at $t = \tau/2$ and $t = 3\tau/2$ (determined from the river difference scheme.) The smoothing operation is as follows :

(i) elevation at the second point of the river at $t = \tau$ is found from the river equation of continuity,

(ii) current at the pivot at $t = 3\tau/2$ is found from the river equation of motion,

(iii) a mean of the currents at the pivot at $t = \tau/2$ and $t = 3\tau/2$ is obtained - yielding a "river" value of current at the pivot at $t = \tau$ (so interpreted)

(iv) the average of this value with the original is taken to give a "smoothed" current at the pivot at $t = \tau$.

Finally, the sea equation of continuity with the revised current value, yields revised values of elevation at the two elevation points of the sea on either side of the first elevation point of the river. A new value of elevation at the latter point is therefore determined by taking the mean of the neighbouring sea elevations as before.

Computation of all the river elevations at $t = \tau$ may now proceed, based on this new elevation input to the river.

The scheme described above is not unique and in fact two other alternative systems of calculation have been formulated, although these have not been put into practice. This emphasises that the work is still in its early stages and much remains to be done in developing and checking it further.

Figure 6 shows one of the alternative schemes. In this the sea grid extends as far as the second river elevation point. The elevation at this point at time τ is found from the river calculation, thence follows a smoothing of the current at the pivot, a revision of the sea elevations at points $I+1$, $I+n+1$, and the subsequent calculation of the river elevations - all at time τ. The two sea elevations on the open boundary are taken equal to the central value - ready to be used in the next step forward in the sea calculation. The open boundary here is, of course, that lying between the river and sea grids.

Looking back on the work so far, it can be truly stated that much of the time has been devoted to the writing and development of the ALGOL program which carries out the computations. Using the limited storage space in the computer to the best advantage has been a major consideration.

Some results which have been obtained using the model for the Thames-southern North Sea region will now be described. There are not enough of these as yet to make any important deductions, but it is probably worthwhile to indicate the present position. Three distinct types of test have been carried out to ascertain the ability of the model to generate tides and surges, and to produce the shallow water effect of interaction between tide and surge. These tests involved studying the response of the model to

(i) wind stress acting over an initially quiescent sea
(ii) co-oscillating tides along the open boundaries and
(iii) a combination of wind stress and tidal co-oscillation.

In generating the surge elevations ζ_s produced by the condition of wind stress over an initially quiescent sea, the following boundary conditions were imposed: Along the open northern boundary of the sea the elevation was permanently zero whilst the southern boundary to the sea and the head of the river were permanently closed to flow. An easterly wind stress was applied over each stream point in the sea and each current section in the river. The stress, a linear function of time, increased from 0-20 dynes/cm^2 (equivalent to a wind speed of 57 m.p.h.) in three hours, stayed constant for a further twelve hours and decreased to zero in the following three hours. Co-disturbance lines showed the resulting depression in sea level along the continental coast produced by off-shore winds, and the pile up of water on the English coast and in the Thames Estuary due to the on-shore winds. The depression in level on the east of the sea was greater than the pile up on the west, since quantities of water were being imbibed by the river. The amplification of the surge as it travelled up the Thames compared favourably with amplification observed when using the one-dimensional model of the Thames Estuary (Rossiter and Lennon 1965). Because the amplification seemed excessive, a second surge case was considered which allowed the wind stress to reach its maximum in 6 hours and thereafter to remain constant. This showed that much of the violent oscillatory motion along the Thames in the first test could be attributed to the near impulsive nature of the stress in that test.

To generate tidal elevations ζ_T corresponding to a spring tide, the M_2 and S_2 co-oscillations along the open boundaries were specified so that the conditions of mean spring high water would occur after the run-in period. Initial tidal conditions of elevation and velocity approximating to mean spring high water were specified, and the spring tidal fresh water flow at the head of the river was specified. A run-in period of two tidal cycles was allowed and calculations were continued for a further 26 hours.

The tidal curves produced were quite smooth (even during the run-in period) and they are shown in figures 7, 8, 9, and 10, as short dashed lines. Good agreement was obtained between computed and observed high water heights and the phase lags of the tide between selected points were in reasonable agreement with observed lags. Computed tidal ranges did not exhibit good agreement with observations. At each section along the river the low water is of the order of 1.5 ft. lower than the observed value and the discrepancy in the time of arrival is of the order of 50 minutes. This can be seen in figure 11 (i, ii) where curves labelled MORASS refer to computed values from the "model of river and shallow sea". Thus the factors which are causing the retardation in the low water and its increase in magnitude, need to be investigated. The discrepancies suggest that there may be insufficient bottom friction, since this would be most noticable at low water when it would permit an increase in tidal amplitude, which in turn would cause a reduction in the speed C of the wave ($C = \sqrt{gh}$) and hence a retarded arrival of the low water.

A combination of wind stress and tidal co-oscillation was achieved by repeating the initial and boundary conditions utilized for the tidal case described above; after the two cycle run-in period, an easterly wind stress, which varied with time as in the first test, was applied over the entire area. Propagation of tide and surge was considered for a 36 hour period.

In the figures 6 to 10, the curves of the tidal elevation ζ_T are the short dashed lines; elevation ζ_{T+S}, due to the co-existence of tide and surge, is shown as an unbroken line. The residual elevation $\zeta_R = \zeta_{T+S} - \zeta_T$ is the long dashed line, and the surge elevation ζ_S is shown as a dotted line.

At section 0, where the depth is 30 ft., tidal curves are quite smooth and regular. A measure of the interaction between tide and surge can be seen by comparing the curves of ζ_R the residual elevation and ζ_S the surge elevation. Such a comparison will also reveal the oscillatory nature of the interaction. Interaction increases up river as can be seen in the curves at section 6, where the depth is 26 ft. The curves at points 640 and 539 show the decrease in the interaction as the depth increases to over 100 ft. at point 539.

The effect of the surge on the heights and times of high waters can also be seen in these figures: on the English coast, the easterly wind stress is providing positive surge conditions which hasten the arrival of the tide. This is due to the increased rate of progression $\sqrt{gh}$ of the free wave due to the increase in the depth; also the decrease in bottom friction permits faster progression of the tide. The opposite effect of negative surge conditions causing a retardation of the tide was seen on the Dutch coast.

Identical wind stress conditions have been imposed over an initially quiescent sea, producing ζ_S and in the presence of a tide producing ζ_{T+S}. Applied over a quiescent sea, oscillatory motion ensued with particularly large ranges of surge elevation ζ_S in the river; however, in the presence of a tide, the oscillations of the residual elevation ζ_R due to surge and interaction were considerably damped, suggesting that the tide has a stabilizing effect on the surge. The fact that the river was closed at the head when producing ζ_S may have contributed to the violent build-up and oscillatory motion of the water. This did not occur when ζ_{T+S} was produced, since then the fresh water flow into the river had been specified.

For practical surge forecasting, the present simple model would require an hour of computer time to predict sea levels for a twenty-four hour period. Although the model has given encouraging results so far, it must undergo several modifications before an accurate numerical reproduction of measured sea levels and currents can be obtained. Investigations must be carried out into the cause of the discrepancies between the computed and observed tidal range; also the model must be refined to include the variations in the direction and magnitude of the wind stress at each grid point of the area, as it occurs in nature.

Acknowledgement

I wish to express my thanks to Mr. N.S. Heaps of the Tidal Institute for presenting this paper at the I.A.P.O. symposium on Hydrodynamical - Numerical Methods in Physical Oceanography in Berne, Switzerland, in September 1967.

J.E.B.

APPENDIX

A brief description of the finite difference schemes for both the river and the sea now follows.

The river is divided into interlacing current and elevation sections. Both sets of sections are numbered serially 0,1,2 ..... L in the direction of increasing y from the mouth $(l = 0)$ to the head $(l = L)$ of the river. Figure 2 shows the array of points where ε is the sectional spacing between adjacent sections with the same name, this distance being equivalent to the longitudinal grid spacing in the sea, and l is an integer which labels the position of the current or elevation section. Calculations of currents are displaced from calculations of elevation by a time interval $\tau/2$. Thus at elevation section fixed by integer l the elevation at time $m\tau$ is denoted by $\zeta^{(R)}_{m,l}$ whilst at the current section fixed by this integer the current at time $(m+\frac{1}{2})\tau$ is denoted by $\bar{q}_{m+\frac{1}{2},l}$

In finite difference form the equations of continuity and motion are expressed as follows:

$$b_{m-\frac{1}{2},l}\left(\zeta^{(R)}_{m,l} - \zeta^{(R)}_{m-1,l}\right) = -\alpha_R \frac{\tau}{\varepsilon}\left(A_{m-\frac{1}{2},l}\,\bar{q}_{m-\frac{1}{2},l} - A_{m-\frac{1}{2},l-1}\,\bar{q}_{m-\frac{1}{2},l-1}\right) \quad \ldots (1)$$

$$\frac{\bar{q}_{m+\frac{1}{2},l} - \bar{q}_{m-\frac{1}{2},l}}{\tau} = -\frac{\beta_R}{\varepsilon}\left(\zeta^{(R)}_{l+1} - \zeta^{(R)}_{l}\right)_m - \lambda_R\,\bar{q}_{m,l}\frac{C_{m,l}}{\varepsilon} - \kappa_R\,\bar{q}_{m,l}\left|\bar{q}_{m,l}\right|\frac{k_l}{H_{m,l}} + \gamma_R\left[\frac{S_s}{H\rho}\right]_{m,l} - \delta_R\frac{H_{m,l}}{\varepsilon}\left[\frac{\partial\rho}{\rho}\right]_l \quad \ldots (2)$$

Here A, H, $\partial\rho/\rho$ and k are evaluated at current sections and b is evaluated at elevation sections. α_R, β_R, γ_R, λ_R, κ_R, δ_R are conversion factors.

$C_{m,l}/\varepsilon$ is the finite difference replacement for $\partial\bar{q}/\partial y$ at current section l at time $m\tau$ written

$$C_{m,l} = \frac{1}{2}\left(\bar{q}_{m+\frac{1}{2},l} + \bar{q}_{m-\frac{1}{2},l+1}\right) - \frac{1}{2}\left(\bar{q}_{m+\frac{1}{2},l} + \bar{q}_{m-\frac{1}{2},l-1}\right)$$

Here bottom friction $S_s = k\rho\,\bar{q}\,|\bar{q}|$ where k is a dimensional constant. Current at the head is obtained from the fresh water flow there, and at section -1 the current is extrapolated from values at sections 0 and 1 so that

$$\bar{q}_{-1} = 2\,\bar{q}_0 - \bar{q}_1$$

Elevation at section 0 is expressed as

$$\zeta^{(R)}_0 = \frac{1}{2}\left(\zeta_{I+1} + \zeta_{I+n+1}\right)$$

In the sea region, the finite difference mesh contains a total of $2p$ parallels of latitude which are numbered serially moving downwards through the grid (fig. 2). Along each parallel of latitude, there are n grid points. Variables p and n set the latitudinal and longitudinal extension of the sea. Elevation and stream points constitute interlacing sub meshes, in which the parallels are labelled $j = 1, 3, 5, \cdots, 2k-1, \cdots, 2p-1$ and $j = 2, 4, 6, \cdots, 2k, \cdots, 2p$, respectively.

The parallel denoted by integer j corresponds to latitude ϕ_j. Grid points of both sub-meshes are numbered serially from left to right along respective parallels of latitude, working downwards through the grid. At the elevation point i take $\zeta = \zeta_i$ and at stream point i take $U = U_i$, $V = V_i$, the notation $F_{m,i}$ meaning $F_i(m\tau)$.

In finite difference form the hydrodynamical equations are expressed as:

$$\frac{U_{m+1,i} - U_{m,i}}{\tau} = -\kappa \frac{U_{m,i}\left|\sqrt{U_{m,i}^2 + V_{m,i}^2}\right|}{(h_i + Z_{m,i})^2} - \Omega_{2k} V_{m,i} - \beta (h_i + Z_{m,i}) \frac{D_{m,i}}{2\Delta\phi} + \gamma F_{m,i}$$

$$\frac{V_{m+1,i} - V_{m,i}}{\tau} = -\kappa \frac{V_{m,i}\left|\sqrt{U_{m,i}^2 + V_{m,i}^2}\right|}{(h_i + Z_{m,i})^2} + \Omega_{2k} U_{m,i} - \frac{\beta (h_i + Z_{m,i})}{2\cos\phi_{2k}} \frac{E_{m,i}}{\Delta\chi} + \gamma G_{m,i}$$

$$\frac{\zeta_{m+1,i} - \zeta_{m,i}}{\tau} = -\frac{\alpha}{\cos\phi_{2k-1}} \left[\frac{B_{m+1,i}}{2\Delta\phi} + \frac{C_{m+1,i}}{2\Delta\chi} \right]$$

Here again α, β, γ, and κ are conversion factors.

On a longitudinal boundary V_i is zero and on a latitudinal boundary U_i is zero. Here Z_i is the elevation at stream point i which is taken to be an average of the elevations at the points surrounding i. At the pivot $Z_i = \frac{1}{2}(\zeta_0^{(R)} + \zeta_1^{(R)})$. The finite difference replacements for $\frac{\partial U\cos\phi}{\partial\phi}$, $\frac{\partial V}{\partial\chi}$, $\frac{\partial\zeta}{\partial\phi}$ and $\frac{\partial\zeta}{\partial\chi}$ viz $\frac{B_i}{2\Delta\phi}$, $\frac{C_i}{2\Delta\chi}$, $\frac{D_i}{2\Delta\phi}$ and $\frac{E_i}{2\Delta\chi}$ are averaged central differences in the sense that

$$B_i = \frac{1}{2}\left[U_{i-n}\cos\phi_{2k-2} - U_i\cos\phi_{2k} + U_{i-n-1}\cos\phi_{2k-2} - U_{i-1}\cos\phi_{2k}\right]$$

$$C_i = \frac{1}{2}\left[V_i - V_{i-1} + V_{i-n} - V_{i-n-1}\right]$$

$$D_i = \frac{1}{2}\left[\zeta_i - \zeta_{i+n} + \zeta_{i+1} - \zeta_{i+n+1}\right]$$

$$E_i = \frac{1}{2}\left[\zeta_{i+1} - \zeta_i + \zeta_{i+n+1} - \zeta_{i+n}\right]$$

At stream points lying on a closed boundary, the gradients in elevation along and across the boundary are found by extrapolation from gradients in the interior of the sea in the neighbourhood of the boundary.

To smooth V at the pivot I (where the current has also been evaluated from the river equations) the following equation is used:

$$V_{m,I} = \frac{1}{2}\left[V_{m,I} - \frac{1}{2}\left(\bar{q}_{m-\frac{1}{2},0} + \bar{q}_{m+\frac{1}{2},0}\right)\left(h_I + \frac{\zeta_{m,1}^{(R)} + \zeta_{m,0}^{(R)}}{2}\right)\right]$$

Along the open boundaries to the sea the tide can be specified as a series of harmonic functions or else elevations at regular intervals of time at each open boundary point may be specified. Also the initial state of motion and displacement of the sea may be specified, or it may be assumed to be quiescent.

Three procedures for evaluating the elevations and currents throughout the river and the sea are now presented. The procedures differ in their approach to joining the one- and two- dimensional schemes at the pivot, where there is a kind of mutual interaction between the motions of

the river and the sea which must be carried through into the calculations.

Scheme A - Figure 5

All elevations and currents at $t = -\tau/2, 0$ are given. Thus in the river at $t = -\tau/2$ there are values of currents $\bar{q}_l$ for $l = -1, 0, 1, 2, \cdots$ and, at $t = 0$ there are values of elevation $\zeta_l^{(R)}$ for $l = 0, 1, 2 \cdots$. In the sea, values of U_i, V_i and ζ_i are known at $t = 0$ at the stream and elevation points respectively. Elevation Z_i at the stream points is evaluated so that the depth mean currents $U_i/(h_i + Z_i)$ and $V_i/(h_i + Z_i)$ may be found. For the river, using the equation of motion, $\bar{q}_l$ is calculated for $l = 0, 1, 2, \cdots, L$ at $t = \tau/2$ then $\bar{q}_{-1} = (2\bar{q}_0 - \bar{q}_1)_{\tau/2}$ is evaluated.

For the sea, using the equations of motion and then of continuity, U_i, V_i, ζ_i are calculated at $t = \tau$.

Then
- $\zeta_0^{(R)} = \frac{1}{2}(\zeta_{I+1} + \zeta_{I+n+1})$ is evaluated at $t = \tau$
- $\zeta_1^{(R)}$ at $t = \tau$ is found from the river equation of continuity
- $\bar{q}_0$ at $t = \frac{3\tau}{2}$ is found from the river equation of motion.
- SMOOTHING: V_I at $t = \tau$ found already from the sea calculations, is reassessed as $(V_I)_\tau = -\frac{1}{2}\left[(\bar{q}_0)_{\tau/2} + (\bar{q}_0)_{3\tau/2}\right]\left[h_I + \frac{1}{2}(\zeta_0^{(R)} + \zeta_1^{(R)})_\tau\right]$ and the mean of this value with the original "sea" value gives the smoothed value for $(V_I)_\tau$
- Using this new value, ζ_{I+1}, ζ_{I+n+1} and $\zeta_0^{(R)} = \frac{1}{2}(\zeta_{I+1} + \zeta_{I+n+1})$ are calculated at $t = \tau$.

River elevations $\zeta_l^{(R)}$ for $l = 1, 2, 3, \cdots$ $t = \tau$ are found from the river equation of continuity.

Elevations along the open boundary at $t = \tau$ are determined from harmonic constants. Thus the cycle from $(-\tau/2, 0)$ to $(\tau/2, \tau)$ is complete.

Scheme B - Figure 5

This scheme assumes that the transverse flow at the pivot is permanently zero, viz $U_I = 0$ and it proceeds from the starting values at $t = -\tau/2, 0$ as before.

River currents at $t = \tau/2$ are calculated as in Scheme A.

For the sea, using the equation of motion and continuity U_i, V_i and ζ_i are found at $t = \tau$ with the exception of $(V_I)_\tau$, $(\zeta_{I+1})_\tau$ and $(\zeta_{I+n+1})_\tau$.

As a first approximation $(V_I)_\tau$ is taken as $(V_I)_\tau = -(\bar{q}_0)_{\tau/2}(h_I + Z_I)_0$

REPEAT
- From the sea equation of continuity ζ_{I+1} and ζ_{I+n+1} are calculated at $t = \tau$, and $\zeta_0^{(R)} = \frac{1}{2}(\zeta_{I+1} + \zeta_{I+n+1})_\tau$ is evaluated.
- From the river equation of continuity $\zeta_1^{(R)}$ is found at $t = \tau$ and from the equation of motion $\bar{q}_0$ is found at $t = 3\tau/2$.
- Then $(V_I)_\tau = -\frac{1}{2}\left[(\bar{q}_0)_{\tau/2} + (\bar{q}_0)_{3\tau/2}\right]\left[h_I + \frac{1}{2}(\zeta_0^{(R)} + \zeta_1^{(R)})_\tau\right]$ is recalculated.

The procedure shown is repeated until convergence of $(V_I)_\tau$ is established. From the sea equation of continuity ζ_{I+1} and ζ_{I+n+1} are calculated at $t = \tau$ using the final value of $(V_I)_\tau$. Elevations along the open boundary at $t = \tau$ are determined from harmonic constants. Also at $t = \tau$, $\zeta_0^{(R)} = \frac{1}{2}(\zeta_{I+1} + \zeta_{I+n+1})_\tau$ is evaluated and $(\zeta_l^{(R)})_\tau$ is found from the river equation of continuity for $l = 1, 2, 3, \cdots, L$. This completes the cycle from $(-\tau/2, 0)$ to $(\tau/2, \tau)$.

Scheme C - Figure 6

The final scheme assumes that the one- and two- dimensional regions meet along an open boundary where it is assumed that $\zeta_I = \zeta_{I+n} = \zeta_1^{(k)}$

All elevations and currents at $t = -\tau/2, 0$ are initially specified. For the river, using the equation of motion, $\bar{q}$ is calculated at $t = \tau/2$ for $l = 0, 1, 2, 3, \cdots$
For the sea, using the equations of motion and continuity, U_l, V_l and ζ_l are found at $t = \tau$ with the exception of ζ_I and ζ_{I+n}
River current at section -1 is evaluated at $\tau/2$ as

$$\bar{q}_{-1} = \frac{1}{2}\left\{\left[\frac{V_{I+1}}{(h+\zeta)_{I+1}}\right]_0 + \left[\frac{V_{I+1}}{(h+\zeta)_{I+1}}\right]_\tau\right\}$$

Then $\zeta_0^{(k)} = \frac{1}{2}(\zeta_{I+1} + \zeta_{I+n+1})_\tau$ is evaluated at $t = \tau$ and $(\zeta_1^{(k)})_\tau$ is obtained from the river equation of continuity.
River current $\bar{q}_0$ at $t = 3\tau/2$ is found from the river equation of motion and is followed by a re-calculation of

$$(V_I)_\tau = \left\{-\frac{1}{2}\left[(\bar{q}_0)_{\tau/2} + (\bar{q}_0)_{3\tau/2}\right]\left[h_I + \frac{1}{2}\left(\zeta_0^{(k)} + \zeta_1^{(k)}\right)_\tau\right] + (V_I)_\tau\right\}/2$$

and a re-calculation of ζ_{I+1} and ζ_{I+n+1} at $t = \tau$ using the equation of continuity. Also V_{I+1} at $t = \tau$ must be re-calculated, and hence $(\bar{q}_{-1})_{\tau/2}$ from the previous equation.
Thus $\zeta_0^{(k)} = \frac{1}{2}(\zeta_{I+1} + \zeta_{I+n+1})_\tau$ at $t = \tau$ is re-assessed and $\zeta_l^{(k)}$ for $l = 1, 2, 3, \cdots, L$ is obtained from the river equation of continuity.

The cycle from $(-\tau/2, 0)$ to $(\tau/2, \tau)$ is completed by putting $\zeta_{I+n} = \zeta_1^{(k)}$ and $\zeta_I = \zeta_1^{(k)}$ and by determining, from harmonic constants, the elevations along the open boundaries at $t = \tau$.

All the calculations of tide and surge which have been completed to date were based on Scheme A above.

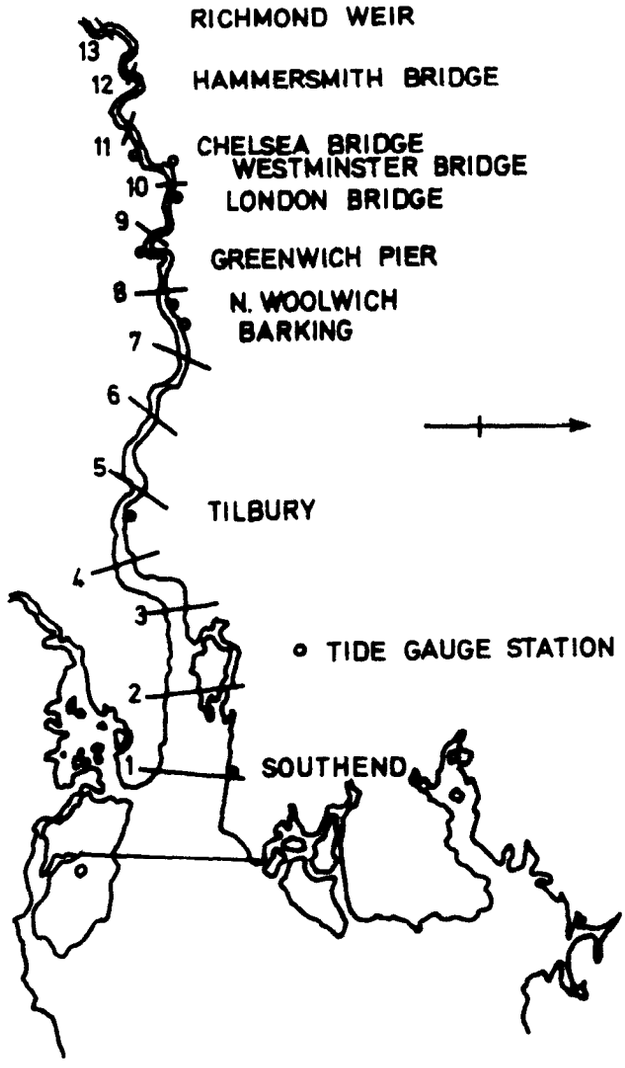

FIGURE 1.

ELEVATION SECTIONS IN THE RIVER THAMES

FIGURE 2.

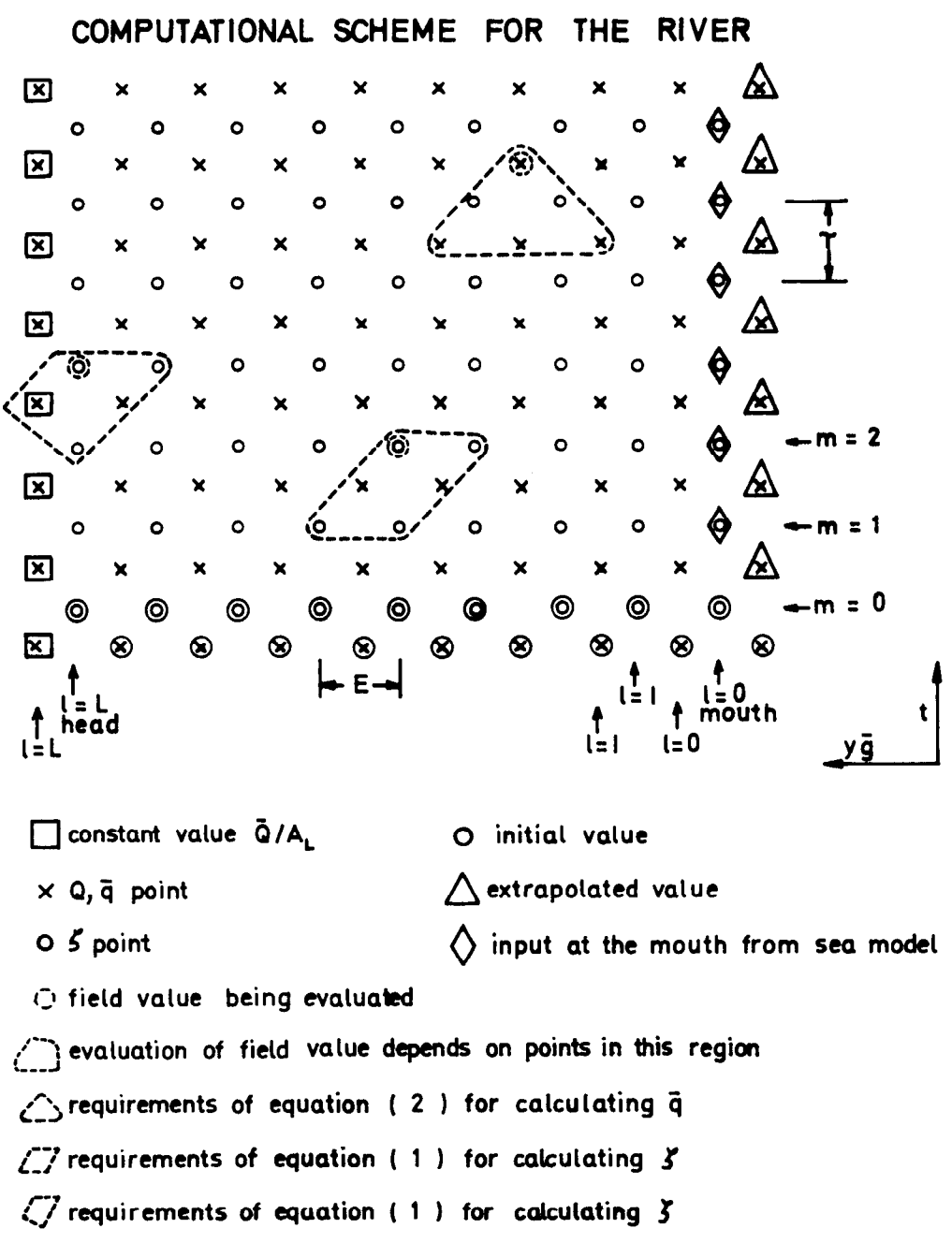
COMPUTATIONAL SCHEME FOR THE RIVER
m = 2
m = 1
m = 0
E
l = L
head
l = L
l = 1
l = 0
mouth
l = 1
l = 0
t
y q̄
constant value Q̄/A_L
initial value
Q, q̄ point
extrapolated value
ζ point
input at the mouth from sea model
field value being evaluated
evaluation of field value depends on points in this region
requirements of equation (2) for calculating q̄
requirements of equation (1) for calculating ζ
requirements of equation (1) for calculating ζ

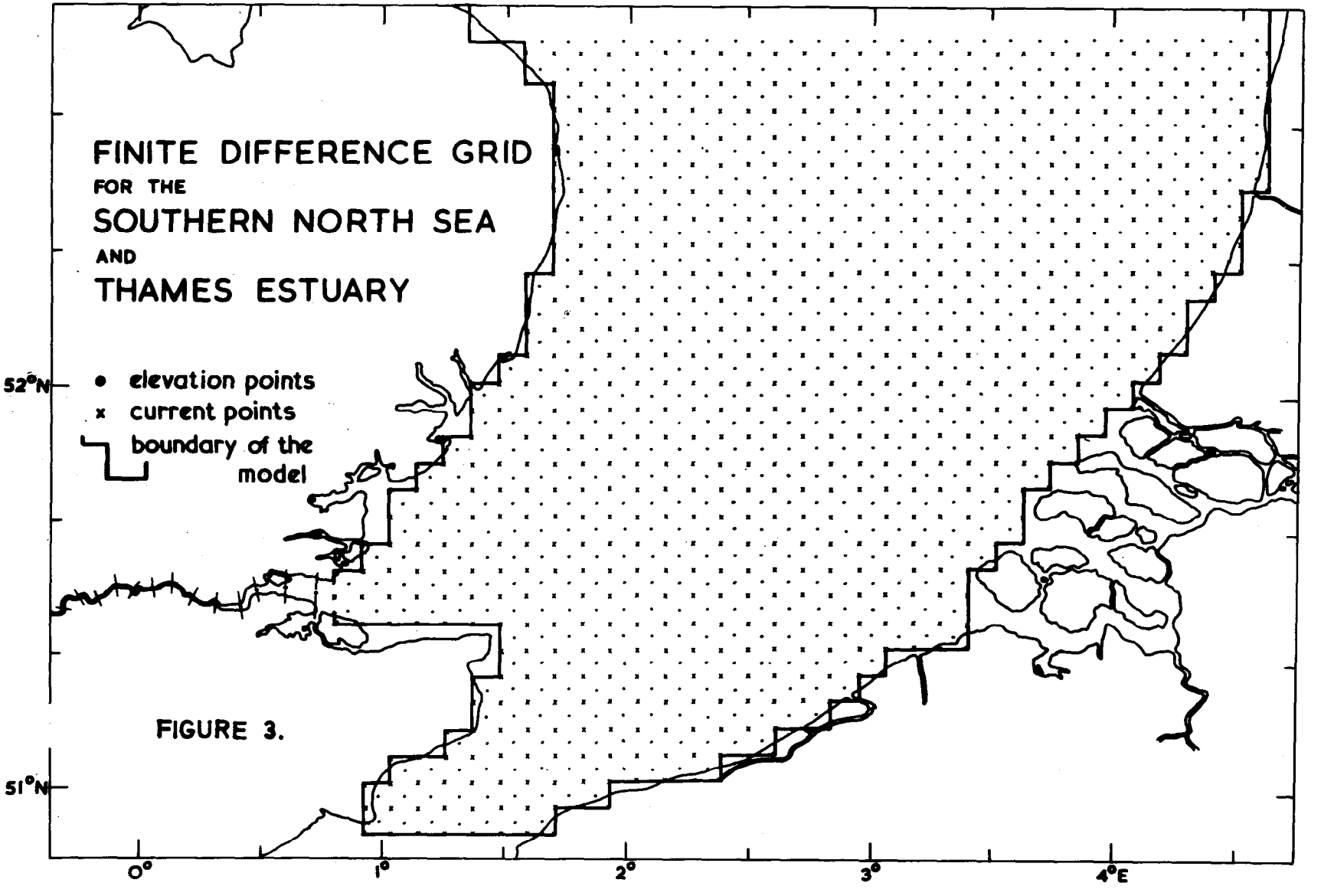
FINITE DIFFERENCE GRID
FOR THE
SOUTHERN NORTH SEA
AND
THAMES ESTUARY
• elevation points
x current points
boundary of the model
52°N
51°N
0°
1°
2°
3°
4°E

FIGURE 3.

FIGURE 4.

PLAN FORM DIAGRAM OF CONNECTION

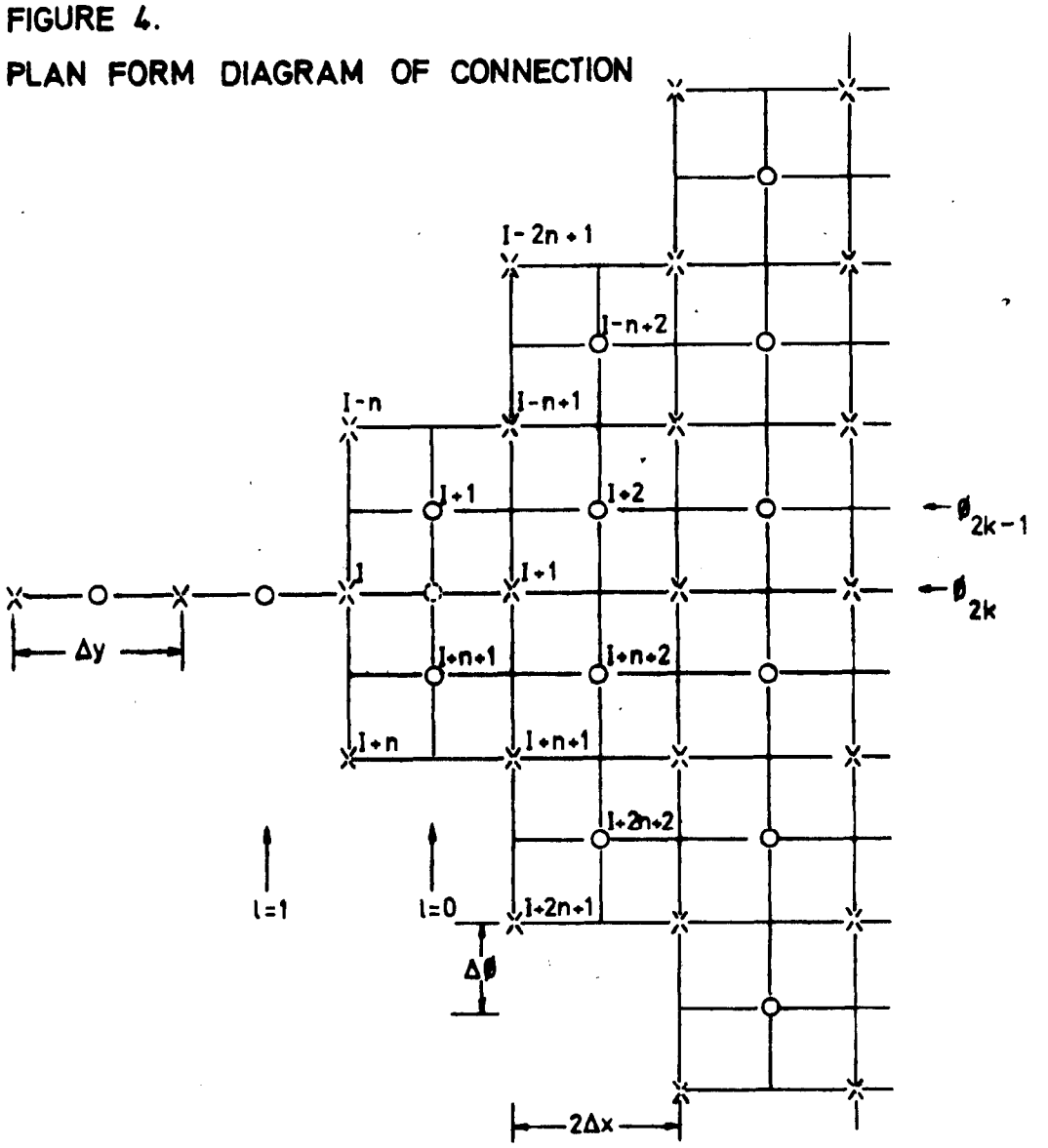

FIGURE 5. COMPOSITE COMPUTATIONAL SCHEME

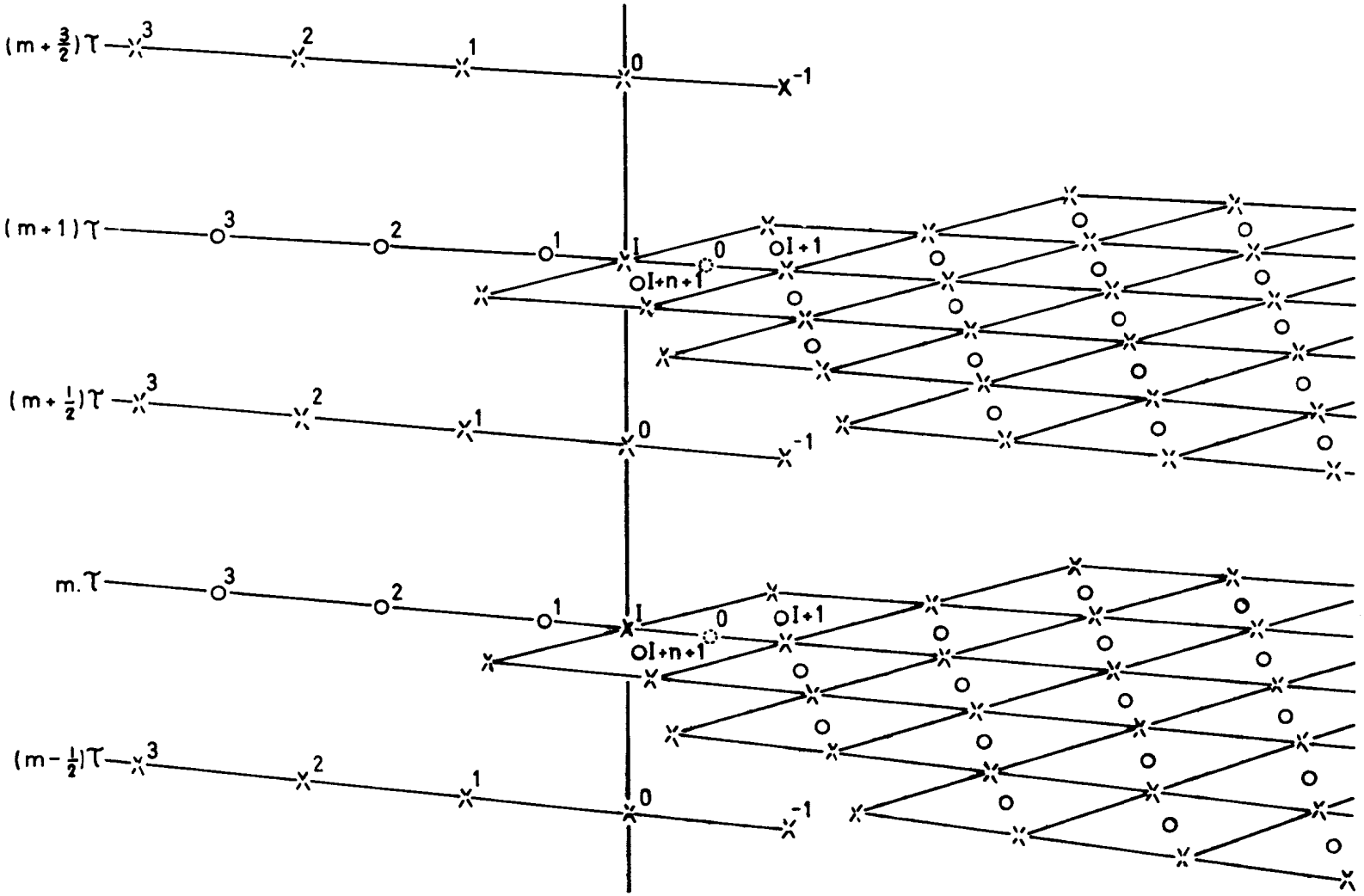

FIGURE 6. ALTERNATIVE COMPOSITE COMPUTATION SCHEME.

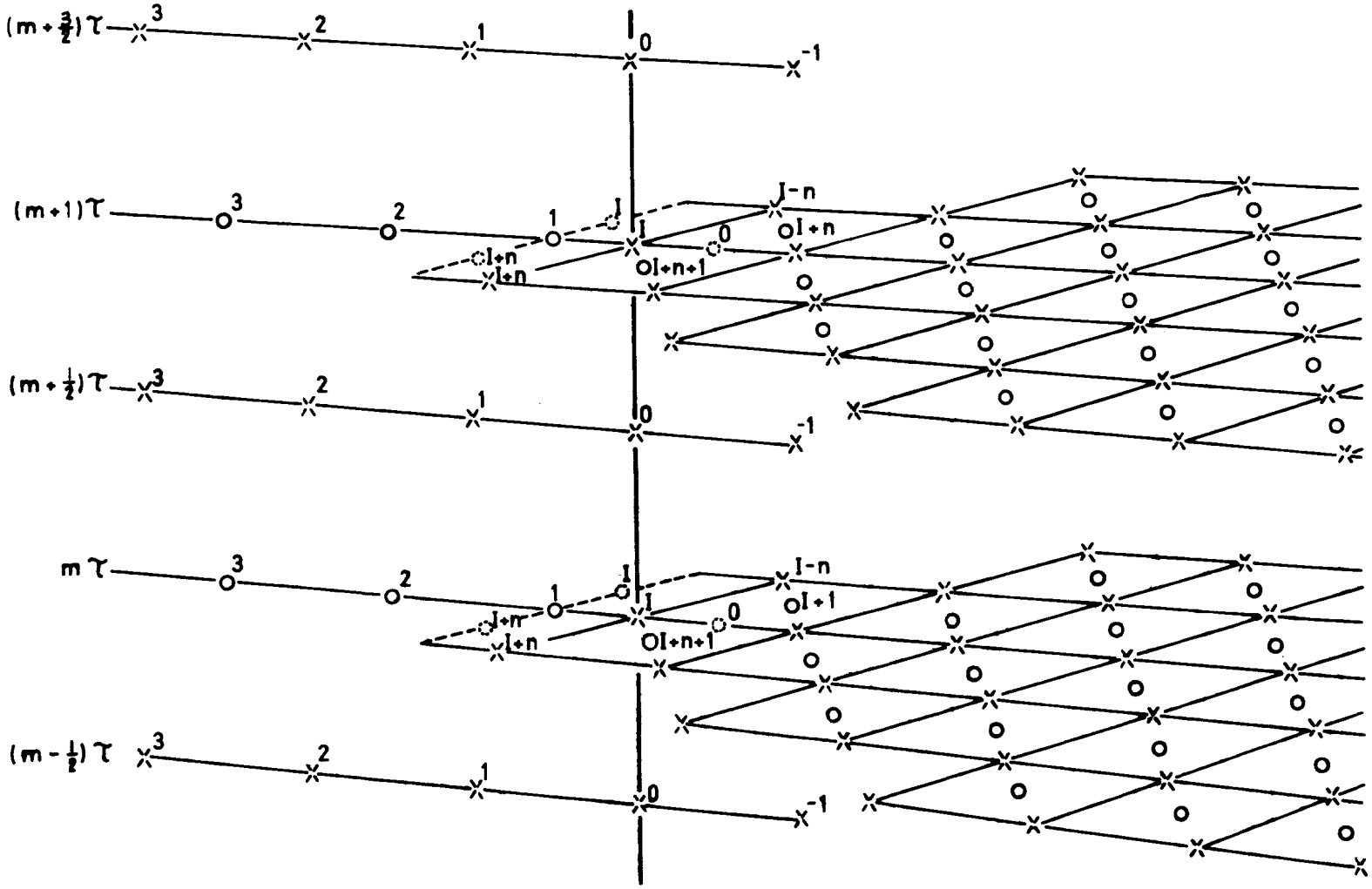

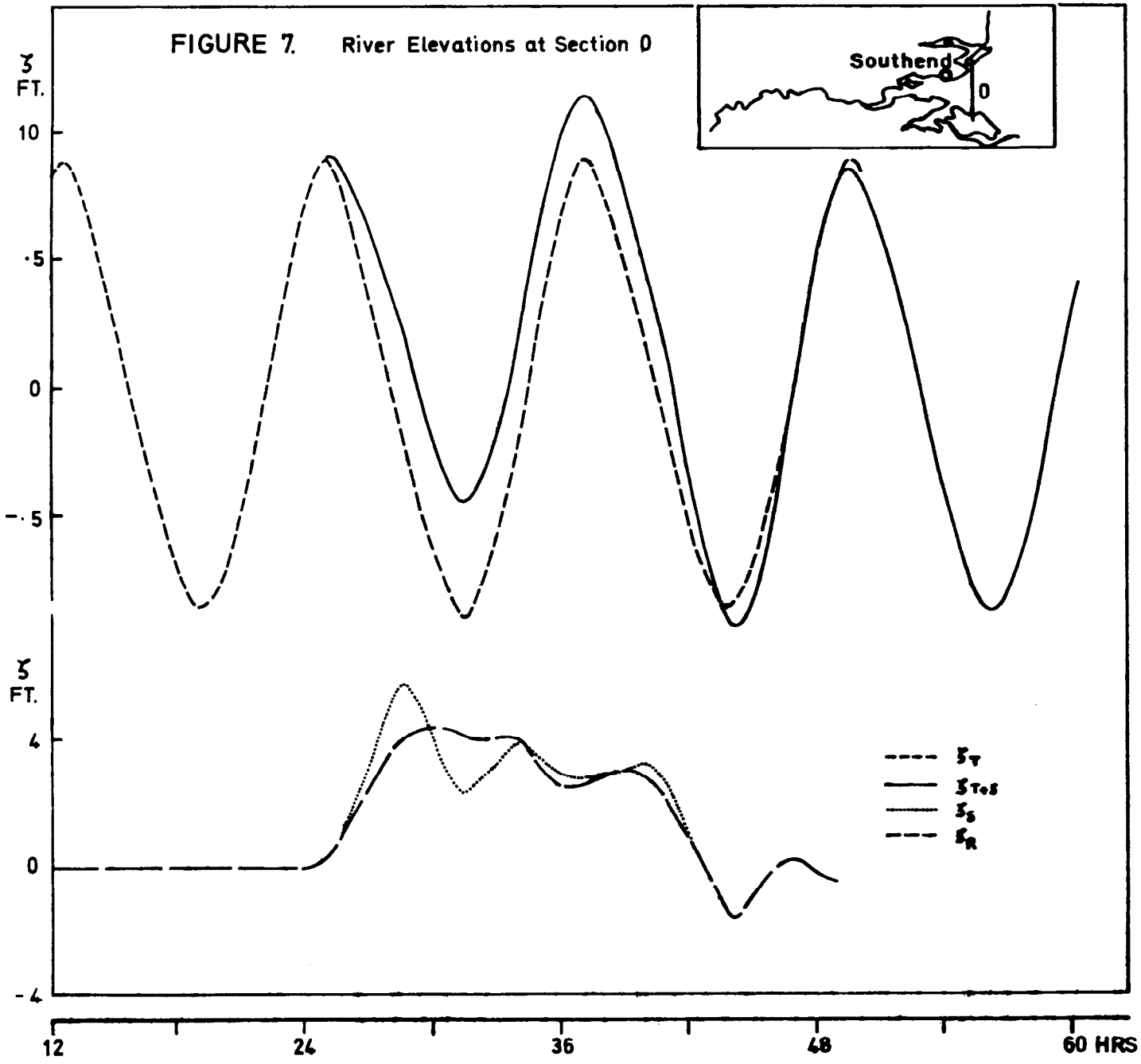
FIGURE 7. River Elevations at Section 0
Southend
0
ζ FT.
10
·5
0
-·5
ζ FT.
4
0
-4
12
24
36
48
60 HRS
ζT
ζT+S
ζS
ζR

FIGURE 8 RIVER ELEVATIONS AT SECTION 6

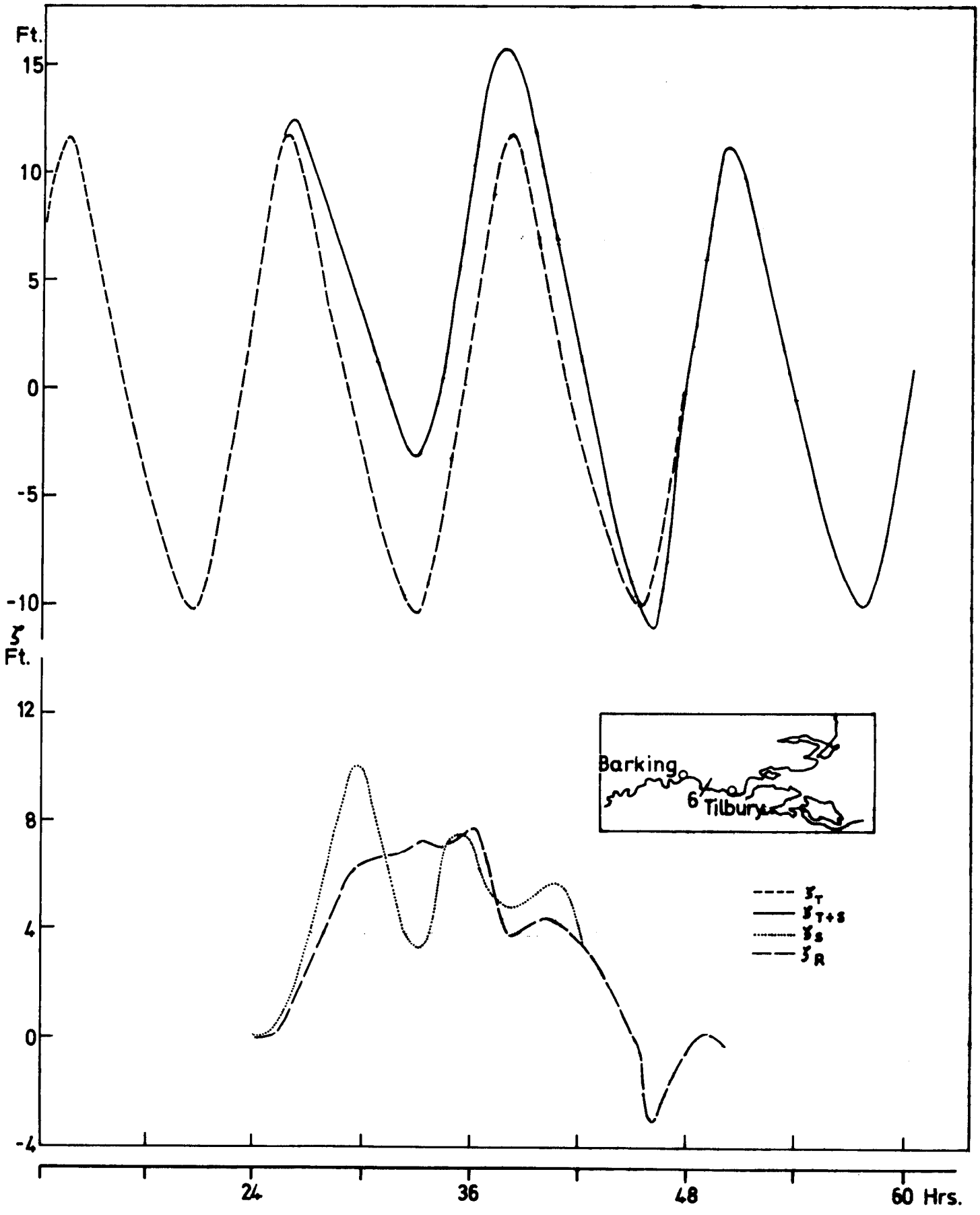

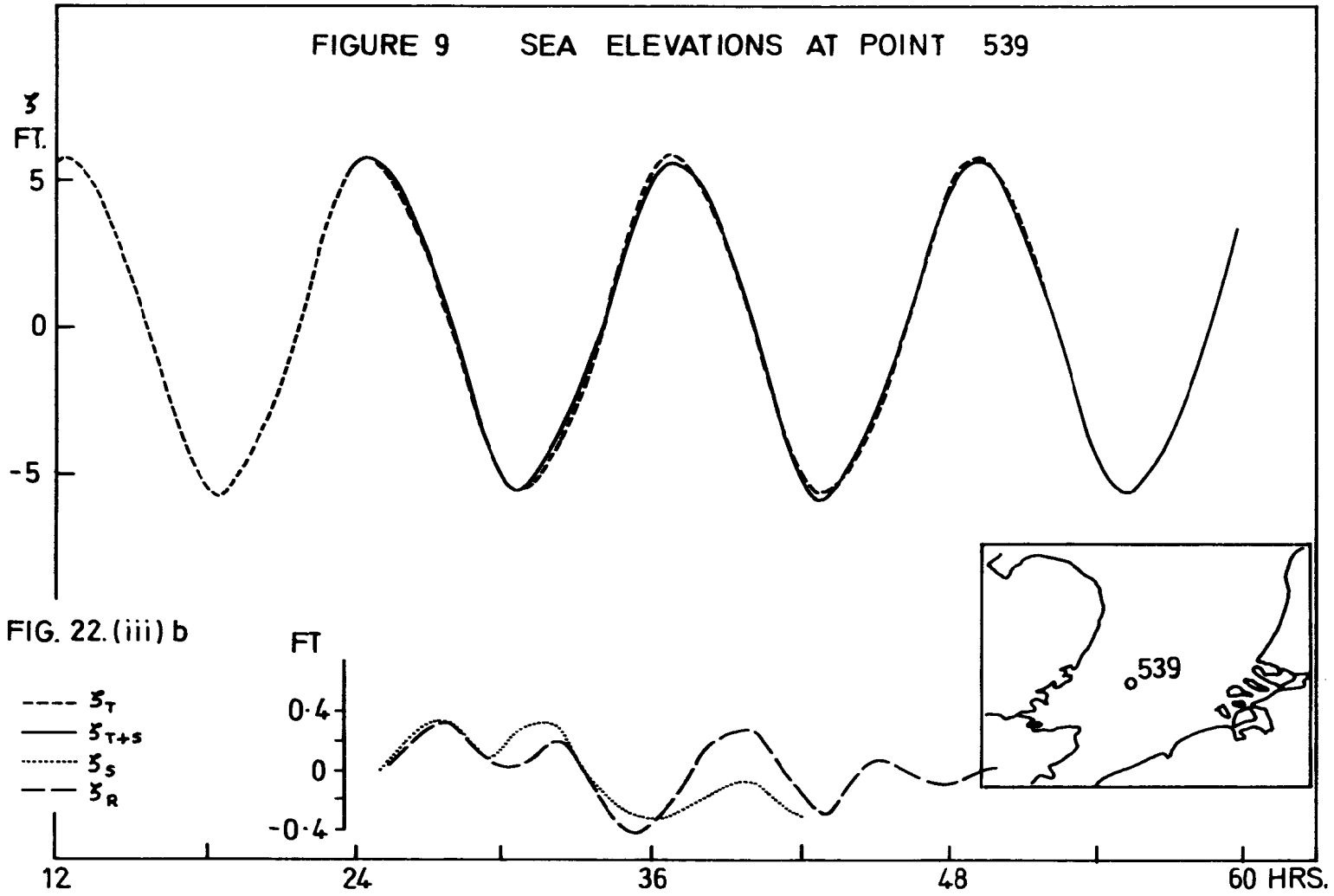
FIGURE 9 SEA ELEVATIONS AT POINT 539
ζ FT.
5
0
-5
FIG. 22.(iii) b
---- ζT
—— ζT+S
..... ζS
— — ζR
FT
0·4
0
-0·4
539
12
24
36
48
60 HRS.

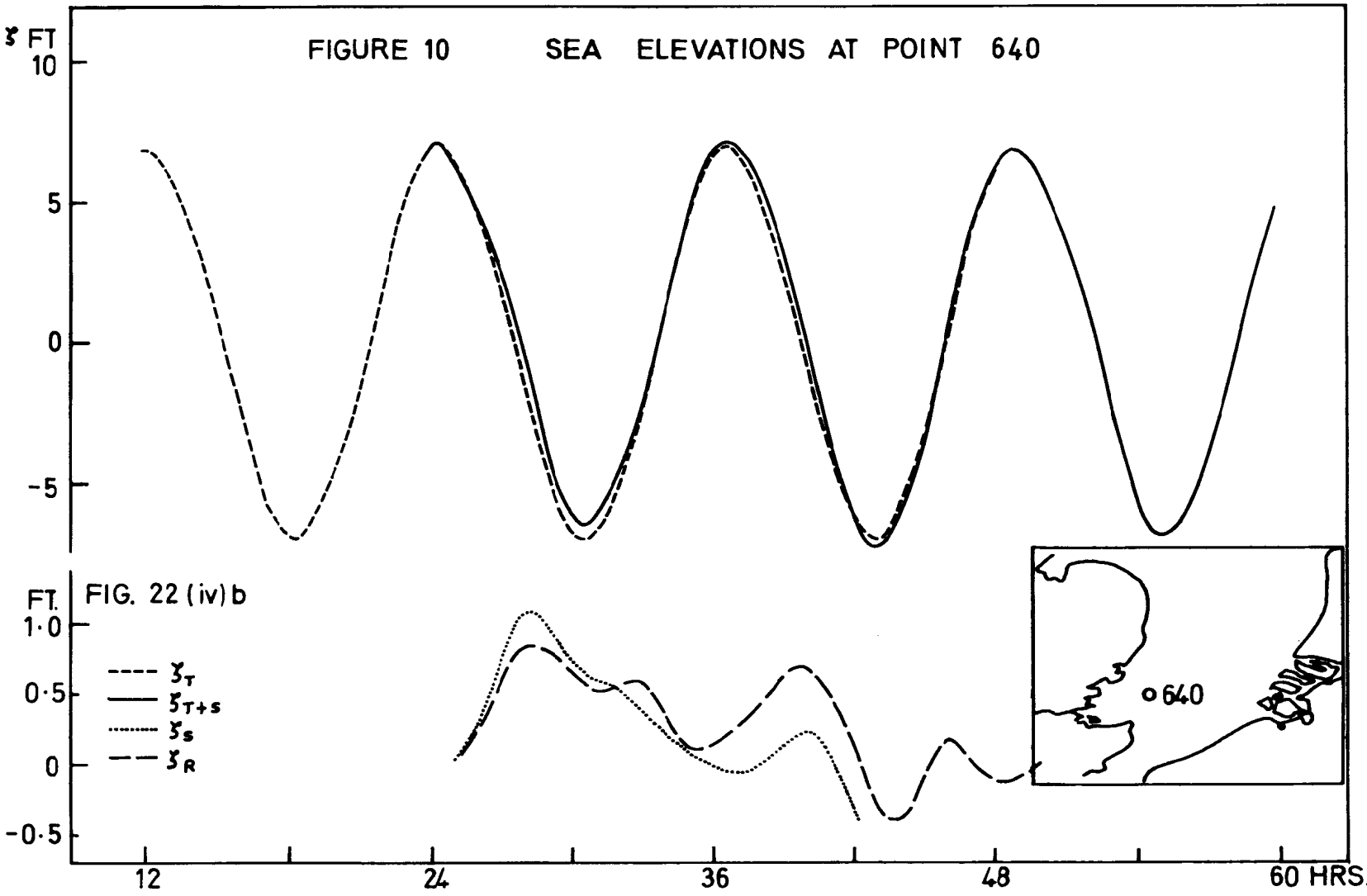
FIGURE 10 SEA ELEVATIONS AT POINT 640
ζ FT
10
5
0
-5
FIG. 22 (iv) b
FT.
1·0
0·5
0
-0·5
ζT
ζT+s
ζs
ζR
o640
12
24
36
48
60 HRS.

FIGURE 11i HEIGHTS OF MEAN HIGH WATER SPRINGS (M.H.W.S.) AND MEAN LOW WATER SPRINGS (M.L.W.S.) ALONG THE THAMES

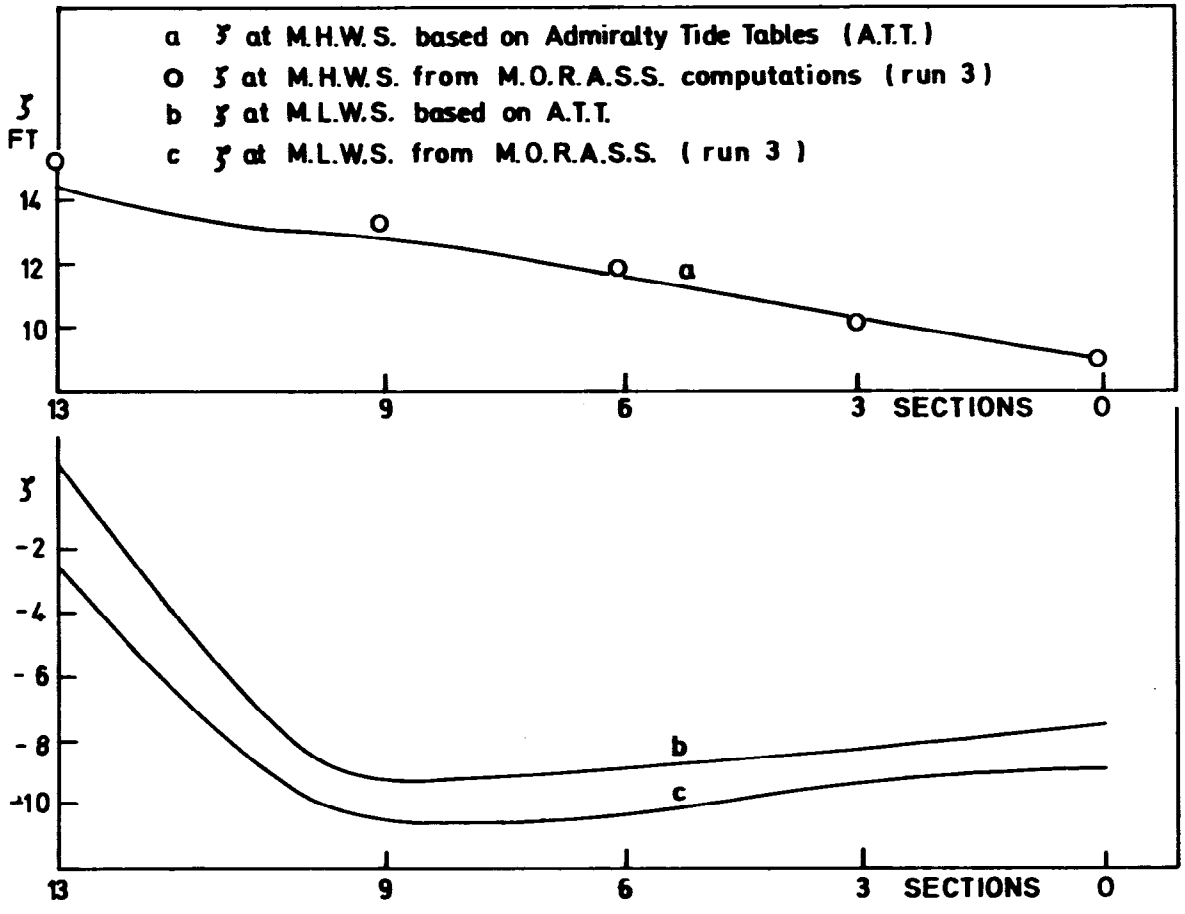

FIGURE 11ii TIMES OF ARRIVAL OF MEAN HIGH WATER SPRINGS (M.H.W.S.) AND MEAN LOW WATER SPRINGS (M.L.W.S.) ALONG THE THAMES.